

Helical dynamo growth at modest versus extreme magnetic Reynolds numbers

Hongzhe Zhou*

*Tsung-Dao Lee Institute, Shanghai Jiao Tong University,
800 Dongchuan Road, Shanghai 200240, People's Republic of China and
Nordita, KTH Royal Institute of Technology and Stockholm University,
Hannes Alfvéns väg 12, SE-10691 Stockholm, Sweden*

Eric G. Blackman†

*Department of Physics and Astronomy, University of Rochester, Rochester, NY, 14627, USA and
Laboratory for Laser Energetics, University of Rochester, Rochester NY, 14623, USA*

(Dated: March 13, 2023)

Understanding large-scale magnetic field growth in astrophysical objects is a persistent challenge. We tackle the long-standing question of how much helical large-scale dynamo growth occurs independent of the magnetic Reynolds number (Rm) in a closed volume. From modest- Rm numerical simulations, we identify a pre-saturation regime when the large-scale field grows independently of Rm , but to an Rm -dependent magnitude. For plausible magnetic spectra however, the analysis predicts the magnitude to be Rm -independent and substantial as $Rm \rightarrow \infty$. This gives renewed optimism for the relevance of closed dynamos and pinpoints how modest Rm and hyper-diffusive simulations can cause misapprehension of the $Rm \rightarrow \infty$ behavior.

Introduction.—Large-scale magnetic fields of many stars, planets, and galaxies require an *in situ* dynamo mechanism to sustain against macroscopic and microscopic diffusion. Plausible dynamo models involve long-lived fields produced by collective motions of stochastic turbulent eddies [1], often studied in the framework of mean-field electrodynamics [2]. Solutions to the suitably averaged mean-field induction equation

$$\partial_t \langle \mathbf{B} \rangle = \nabla \times (\langle \mathbf{U} \rangle \times \langle \mathbf{B} \rangle + \mathcal{E}) + \eta \nabla^2 \langle \mathbf{B} \rangle \quad (1)$$

are sought, where $\mathbf{B} = \langle \mathbf{B} \rangle + \mathbf{b}$ is the total magnetic field measured in Alfvén units, $\langle \cdot \rangle$ is an average over a scale assumed to be much larger than the turbulent forcing scale, and η is the magnetic diffusivity. We use lower case \mathbf{b} to indicate the contribution to \mathbf{B} with zero mean, and similar constructions for the magnetic vector potential \mathbf{A} and velocity \mathbf{U} . For statistically homogeneous and isotropic, kinetically helical turbulence, the turbulent electromotive force (EMF) \mathcal{E} contains a term $\alpha \langle \mathbf{B} \rangle$ that can amplify $\langle \mathbf{B} \rangle$ [2–5]. The increasing Lorentz force on the flow eventually quenches the dynamo.

A long-debated question is whether the quenching becomes more severe at higher magnetic Reynolds numbers Rm [6–13]. In the “dynamical quenching” (DQ) formalism, gradients of $\langle \mathbf{B} \rangle$ are required for it to grow, and the dynamo quenching is controlled by the conservation of magnetic helicity [14–19]. In this formalism, significant growth of $\langle \mathbf{B} \rangle$ occurs during an Rm -independent regime, after which Rm -dependent saturation occurs. The field strength can reach super-equipartition values, but only on a resistively long time scale [17, 20, 21]. Although resistive time scales are appropriate for planets, large Rm

renders the resistive growth time scale too long for many stellar and galactic contexts. This raises the question of how strong $\langle \mathbf{B} \rangle$ gets before Rm dominates the evolution.

A substantial Rm -independent regime has not yet been definitively identified in simulations. This, and the often impractically long time scale for the fully saturated phase, make it challenging to understand the origin of large-scale fields in astrophysical flows from helical dynamo. Solutions to this problem include helicity fluxes [e.g., 16, 22–26] and anisotropic forcing [27]. See Ref. [28] for a comprehensive review, and also Refs. [29–32].

In this Letter, we investigate whether an Rm -independent regime can exist before the very long resistive phase. The helical dynamo in a closed system consists of three distinct temporal stages: (i) a fast small-scale dynamo (SSD) that grows on turbulent time scales, (ii) a large-scale dynamo (LSD) that is $\mathcal{O}(10)$ times slower than the SSD, and (iii) a growth driven by magnetic helicity dissipation that operates on resistive time scales. At very early times when the magnetic energy is negligible to the kinetic energy at all scales, the SSD and LSD phases can be described in a unified framework [33–35]. Once the SSD nearly saturates, LSD takes over and potentially operates independently of resistivity [36, 37]. The resistive phase dominates once the LSD saturates [17, 20, 38, 39] Here we answer the question: does the LSD phase amplify $\langle \mathbf{B} \rangle$ to an Rm -independent value before dynamical quenching transitions to the resistively limited asymptotic phase? We call the regime whose Rm dependence we assess as the “pre-quenched” (PQ) regime, a definition to be further clarified later.

To answer our question from numerical simulations is challenging without careful interpretation, because the time scales of the LSD and the resistive phases are poorly separated at moderate values of Rm available. Instead of using time to delineate dynamo phases, here we employ a new dynamo tracker which records how much the

* hongzhe.zhou@sjtu.edu.cn

† blackman@pas.rochester.edu

dynamo driver has been quenched. At each quenching level, we analyze individually the Rm-dependence of the LSD growth rate and the field strength. We then discuss the distinct implications of our analysis for the modest Rm values obtainable in the simulations versus the implications for asymptotically large Rm.

Methods.—We perform compressible magnetohydrodynamics simulations with an isothermal equation of state using the PENCIL CODE [40, 41]. The velocity is driven in a $(2\pi)^3$ -periodic box using positively helical plane waves at a fixed forcing wave number k_f , but with random phases and directions at each time step. The vector potential \mathbf{A} is solved in the resistive gauge (i.e., the scalar potential is $\phi = -\eta \nabla \cdot \mathbf{A}$), but periodic boundary conditions ensure that the magnetic helicity is gauge invariant. For all runs, we use $k_f = 4$ and Mach numbers $\text{Ma} \simeq 0.1$. The Reynolds numbers $\text{Re} = u_{\text{rms}}/\nu k_f$ (with u_{rms} being the instantaneous root-mean-square velocity and ν being the viscosity) are kept roughly constant, $\simeq 5$, and the magnetic Prandtl number $\text{Pm} = \nu/\eta$ is varied from 1 to 100. This isolates the Rm dependence from that of Re.

We consider only the helical part of the magnetic field, as it is most relevant to the LSD. Although the current helicity spectrum \mathcal{H}^C is always gauge-independent, we formulate the equations using the magnetic helicity spectrum \mathcal{H}^M for convenience. For the present boundary conditions, the two are related by $\mathcal{H}^C = k^2 \mathcal{H}^M$ where k is the wave number. We normalize energy and helicity spectra such that integration over all wave numbers yields the energy or helicity density. We then decompose the large- and small-scale magnetic helicity densities as

$$\int \mathcal{H}_i^M dk = s_i k_i^{-1} \int k |\mathcal{H}_i^M| dk, \quad (2)$$

where $i = 1, 2$ denote large-scale ($k < k_f$) and small-scale ($k \geq k_f$) modes respectively, $s_i = \int \mathcal{H}_i^M dk / \int |\mathcal{H}_i^M| dk$ is the mean handedness, and $k_i = \int k |\mathcal{H}_i^M| dk / \int |\mathcal{H}_i^M| dk$ is the mean wave number of the helical fields. Note that $s_i \in [-1, 1]$ and $k_i > 0$. The non-dimensional energy density of the large-scale helical field is $\tilde{E}_L = u_{\text{rms}}^{-2} \int k |\mathcal{H}_1^M| dk$. We define dimensionless time as $\tilde{t}(t) = \int_0^t u_{\text{rms}}(t') k_f dt'$ which is monotonic in t , and reduces to $\tilde{t} = t u_{\text{rms}} k_f$ for constant u_{rms} . We also define the dimensionless exponential growth rate $\tilde{\gamma} = \text{dln } \tilde{E}_L / \text{d}\tilde{t}$.

LSD growth rate versus Rm—For statistically isotropic and homogeneous turbulence, the turbulent EMF in Eq. (1) takes the form $\mathcal{E} = \alpha \langle \mathbf{B} \rangle - \beta \nabla \times \langle \mathbf{B} \rangle$. The turbulent diffusivity is $\beta = \tau u_{\text{rms}}^2 / 3$, and $\tau = 1/u_{\text{rms}} k_f$. In the DQ formalism, $\alpha = \alpha_k + \alpha_m$. Here

$$\alpha_k = -\frac{1}{3} \left\langle \int_0^t \mathbf{u}(t) \cdot \nabla \times \mathbf{u}(t') dt' \right\rangle \simeq -\frac{1}{3} \epsilon u_{\text{rms}} \quad (3)$$

is the kinetic contribution, and the magnetic contribution

$$\alpha_m = \frac{1}{3} \left\langle \int_0^t \mathbf{b}(t) \cdot \nabla \times \mathbf{b}(t') dt' \right\rangle \simeq \frac{1}{3} \left(\int k \mathcal{H}_2^M dk \right)^{1/2} \quad (4)$$

grows by DQ [14, 15, 17] and is related to the small-scale current helicity multiplied by a correlation time. In Eq. (3), we have assumed the velocity field to be fully helical, which is consistent with our simulations. We also introduced a factor ϵ to capture the possible deviation of the correlation time between \mathbf{u} and its curl, from the eddy turnover time $1/u_{\text{rms}} k_f$. Measuring ϵ can be method-dependent and so we treat it as a free parameter. We shall see that $\epsilon = 0.85$ is sufficient to explain simulations, and more crucially, it has no influence on the implications on the Rm-dependence of helical LSDs.

In the DQ formalism, α_m grows in time, offsets α_k , and eventually quenches the dynamo. We thus define $\chi \equiv -\epsilon \alpha_m / \alpha_k$ as the DQ factor, which is roughly the normalized current helicity. It contains no free parameter and is calculable from simulations. The measured value of χ grows nearly monotonically in time with fluctuations. In what follows, any quantity taken at $\chi = \chi'$ is meant to be its average over the interval $\chi \in [\chi' - \delta', \chi' + \delta]$ with $\delta = \min\{0.2\chi', 0.05\}$, unless otherwise specified.

For sufficiently large Rm, SSD is excited at early times and the growth of the large-scale modes is dominated by nonlinear inter-mode interactions rather than the interaction with the velocity field through the α effect. The value of χ at which the large-scale modes are dominated by LSD is empirically found to be $\chi \simeq 0.1$, as determined by two measurements: (i) The mean-to-rms ratio, $\langle B \rangle^2 / B_{\text{rms}}^2$, remains constant at $\chi \leq 0.1$ for all runs, which is a signature SSD feature; (ii) The SSD phase efficiently amplifies small-scale fields but with low fractional magnetic helicity, e.g. an average value of 0.05 for the simulation run at $\text{Rm} = 259$. Thus $\chi > 0.1$ is primarily a result of the helical LSD.

For a helical LSD without a mean flow (i.e., an α^2 dynamo), the energy growth rate of the mode at wave number k_1 is $\gamma = 2|\alpha|k_1 - 2(\beta + \eta)k_1^2$ [28]. Using the eddy turnover rate $u_{\text{rms}} k_f$ for normalization, we have [42]

$$\tilde{\gamma} = \frac{\gamma}{u_{\text{rms}} k_f} = \frac{2k_1}{3k_f} (\epsilon - \chi) - \left(\frac{2}{3} + \frac{2}{\text{Rm}} \right) \left(\frac{k_1}{k_f} \right)^2, \quad (5)$$

where $\text{Rm} = u_{\text{rms}}/\eta k_f$ is the instantaneous magnetic Reynolds number. The LSD initially operates kinematically when $\chi \ll 1$, but is then dynamically quenched by χ due to the growing small-scale current helicity. The maximal value χ can obtain is analytically determined by $\tilde{\gamma} = 0$ to be $\epsilon - k_1/k_f$ when $\text{Rm} \rightarrow \infty$. For the runs with large Rm (A4 to A6), we have approximately $\epsilon = 0.85$ (see Fig. 1(a) and also the next paragraph), and hence the LSD regime for which $\chi \in [0.1, 0.6]$ quantitatively demarks the PQ regime whose Rm dependence we will assess. Resistive diffusion of magnetic helicity reduces the growth rate of χ and thus slows the magnetic back-reaction on the LSD, but does not directly show up in the LSD growth rate. Hence at any given χ during the LSD phase, the LSD growth rate can become Rm-independent at lower Rm than the value at which the mean-field strength becomes Rm-independent. We focus

on $\tilde{\gamma}$ here and discuss the influence of resistivity on the field strengths later.

Eq. (5) is the theoretical expectation of the LSD growth rate. To validate it from simulations, it is more convenient to define an LSD efficiency $\sigma = \epsilon - \chi$ and express this in terms of $\tilde{\gamma}$ using Eq. (5),

$$\sigma = \frac{3k_f}{2k_1} \tilde{\gamma} + \left(1 + \frac{3}{\text{Rm}}\right) \frac{k_1}{k_f}. \quad (6)$$

The right side is directly measured in simulations as plotted in Fig. 1(a), with varying Rm for different colors. Overall, the measured values of σ at $\chi \in [0.1, 0.5]$ can be well described by the theoretical expectation $\epsilon - \chi$, with $\epsilon \in [0.85, 1]$, as indicated by the two black dashed lines. This implies a modest 15% deficit in the correlation time between \mathbf{u} and its curl (which enters α_k) than that between \mathbf{u} and itself (which enters β), and might explain the sub-maximal LSD efficiency of Ref. [37].

The agreement between measured values and theoretical expectation of σ validates Eq. (5), and thus justifies that (i) the DQ formalism correctly describes the α^2 dynamo, and (ii) the LSD growth rate is asymptotically independent of Rm when $\text{Rm} \gg 1$. To see the latter point, notice that on the right of Eq. (5) the only two Rm-dependent quantities are Rm itself and k_1 . The k_1 is initially the value $\sim k_f/2$ which maximizes $\tilde{\gamma}$. Later, k_1 decreases to the lowest wave number available in the system, and this evolution may depend on Rm. But overall, k_1 always changes by a factor of $k_f L/4\pi$ if L is the length scale of the system, which is Rm-independent. Hence the Rm-dependence of $\tilde{\gamma}$ introduced by k_1 is quite weak and $\tilde{\gamma}$ will not decrease to some resistively small value. Indeed, Fig. 1(a) shows that σ , and hence $\tilde{\gamma}$, become Rm-independent once $\text{Rm} \gtrsim 130$. An Rm-independent growth rate was previously reported at $\text{Rm} \gtrsim 500$ [37], but here we provide evidence at lower Rm.

Rm-dependent field strengths in simulations— Although the LSD growth rate is verified to be independent of Rm for $\text{Rm} \rightarrow \infty$, the simulated values of \tilde{E}_L decrease with increasing Rm at fixed χ . To quantify this, we define an exponent $p(\chi)$ by fitting the power-law $\tilde{E}_L(\chi, \text{Rm}) \propto \text{Rm}^{p(\chi)}$. We find that $p \simeq -0.5$ for all $\chi \in [0.01, 0.6]$, indicating that during the SSD phase and at all stages of the LSD, the mean-field energy decreases with increasing Rm. We now explain this dependence.

\tilde{E}_L can be inferred from the total magnetic helicity without integrating the growth equation. Consider the case where the volume-averaged magnetic helicity is zero initially, but later gains $\Delta H = H_1^M + H_2^M$ due to resistive diffusion, where $H_{1,2}^M$ are the average magnetic helicity of the large- and small-scale fields, respectively. Using Eq. (2) we have $H_1^M = s_1 k_1^{-1} \tilde{E}_L u_{\text{rms}}^2$, and therefore

$$\tilde{E}_L(\chi, \text{Rm}) = -\frac{k_1}{s_1} \frac{H_2^M}{u_{\text{rms}}^2} + \frac{k_1 \Delta H}{s_1 u_{\text{rms}}^2}. \quad (7)$$

We denote the two terms on the right of Eq. (7) by T_D and T_R , respectively, so that $\tilde{E}_L = T_D + T_R$. Note that

T_R is from the resistive loss of magnetic helicity but T_D is purely dynamic. The resistive term does not amplify the large-scale field directly, but slows the growth of χ , thereby weakening the back-reaction and allowing more large-scale growth. The ratio T_D/\tilde{E}_L determines whether resistive effects dominate and this is to be assessed below.

For all runs at all times, the magnetic fields near the resistive wave number have positive magnetic helicity, whilst those at the lowest wave numbers have negative helicity. Hence $\Delta H < 0$ and $s_1 < 0$ always. As we discuss in detail in Supplemental Material [42], $H_2^M < 0$ during the SSD phase, and hence $T_D/\tilde{E}_L < 0$ initially. In what follows we focus on the LSD phase when $H_2^M > 0$, the period during which T_D and T_R are both positive.

The evolution of T_D/\tilde{E}_L is shown in Fig. 1(b). The LSD starts to dominate the field growth at k_1 at $\chi \gtrsim 0.1$, and its back-reaction on the small scales grows T_D . By the time $\chi = 0.6$ which is close to the end of the LSD regime, Eq. (7) determines how much the LSD has benefited from resistive contributions. That $T_D < T_R$ implies that the LSD quenching is still weakened substantially by the resistive dissipation of small-scale current helicity, and therefore the PQ regime depends strongly on Rm. This is why \tilde{E}_L decreases with increasing Rm at fixed χ .

Implications for higher Rm.—Fig. 1(b) shows that by $\chi = 0.6$, the fractional contribution from T_D increases with increasing Rm, but stops increasing for the highest Rm run A6. We now describe why this apparent saturation may not apply for much larger Rm, and why T_D might actually dominate at $\chi = 0.6$ as $\text{Rm} \rightarrow \infty$ and become Rm-independent.

Since $T_R \propto \Delta H$ and is negligible during the LSD phase in the $\text{Rm} \rightarrow \infty$ limit, the necessary condition for an Rm-independent PQ regime is $dT_D/d\text{Rm} \rightarrow 0$ as $\text{Rm} \rightarrow \infty$. In the LSD phase, the small-scale magnetic helicity spectrum \mathcal{H}_2^M is of one sign, so we write $T_D = -s_2 k_1 \chi^2 / s_1 k_2$. Since $|s_{1,2}| \simeq 1$ and k_1 is bounded from below, an Rm-independent PQ regime requires k_2 to depend at most weakly on Rm at fixed χ , which is determined by the magnetic helicity spectrum as explained below.

Consider a magnetic helicity spectrum, $\mathcal{H}_2^M(k) \propto k^{-q}$ in the inertial range. This is appropriate for $\text{Pm} < 1$ flows. Using Eq. (2) for k_2 , we then have that $k_2/k_f = F(q-1)/F(q)$, where $F(x) = \int_1^r x^{-q} dx$, and r is the ratio between the dissipative scale of the helical fields and k_f . When $\text{Rm} \rightarrow \infty$, we have $r \gg 1$, so that $k_2/k_f = (q-1)/(q-2)$ when $q > 2$, but diverges for $q \leq 2$. Hence an Rm-independent PQ regime arises if $q > 2$.

For $\text{Pm} > 1$ flows whose magnetic energy and helicity spectra may have broken power laws at $k \geq k_f$, the conditions for an Rm-independent PQ regime become (i) a $q > 2$ range exists, and (ii) the wave number above which $q > 2$ does not increase with increasing Rm. Such evidence is indeed observed from our $\text{Pm} \geq 1$ simulations. For the two highest-Rm runs (at $\text{Rm} \simeq 250$ and 500), we find that the wave numbers at which $q - 2$ changes sign are both $\simeq 2k_f$ and do not scale with Rm. This is consistent with previous indications that the peak wave

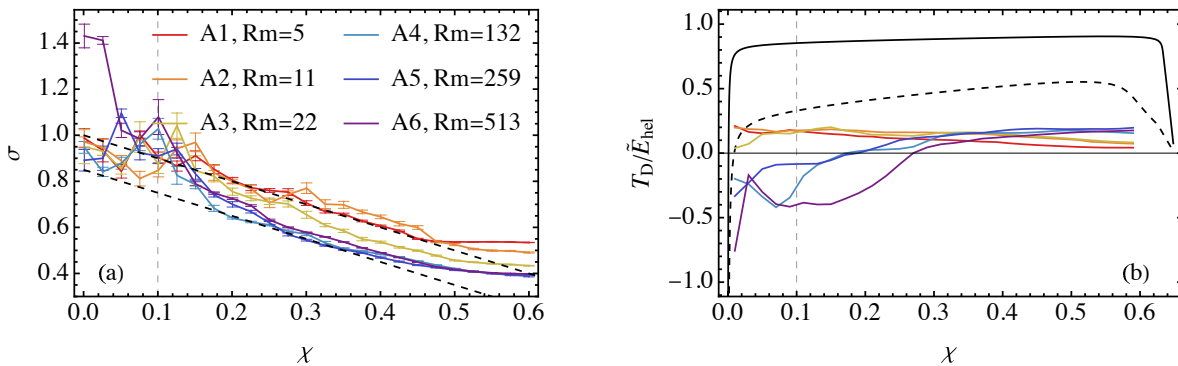


FIG. 1. Rm-independent growth and Rm-dependent field strength in helical LSDs. In both panels, the vertical dashed line at $\chi = 0.1$ indicates the start of the LSD phase. (a) Measured values of LSD efficiency σ [Eq. (6)] versus the dynamical quenching factor χ for different Rm. The two black dashed lines indicate the theoretical expectation $\sigma^{\text{th}} = \epsilon - \chi$ with different ratios of the time scales of α_k and β : $\epsilon = 1$ (upper) and $\epsilon = 0.85$ (lower). The LSD growth rate becomes independent of Rm for runs A4 to A6, i.e., when $Rm \geq 130$. (b) Fractional contributions to \tilde{E}_L from the dynamical term, T_D/\tilde{E}_L , from the simulation data (colored) and the theoretical LSD model (black). Hence $T_R/\tilde{E}_L = 1 - T_D/\tilde{E}_L$ decreases with increasing Rm but still dominates when $Rm \simeq 500$, leading to Rm-dependent field strengths in simulations. Two theoretical LSD curves are shown for $Rm = 2500$ with $q = 8/3 > 2$ (solid) and $q = 1 < 2$ (dashed).

number of the magnetic energy spectrum for large-Pm SSDs remains Rm-independent for large Rm from both theory [33] and simulation [43]. Hence, our simulations imply an Rm-independent PQ regime for $Pm \geq 1$ flows.

Fig. 1(b) shows two theoretical predictions for the fractional dynamical contribution T_D/\tilde{E}_L at $Rm = 2500$ in black, using a three-scale model (see Supplemental Material [42]), with $q = 8/3$ implying Rm-independent quenching and $q = 1$ implying Rm-dependent quenching. For the latter, the resistive terms still contributes nearly half of the large-scale helical field, implying an Rm-dependent field strength during the PQ phase. Near the fully quenched state at $\chi \simeq \epsilon - k_1/k_f$, the LSD growth rate has become smaller than the resistive loss rate of the small-scale magnetic helicity, and therefore the growth of the large-scale field is always dominated by the resistive term for any finite Rm. This leads to the decay of T_D/\tilde{E}_L at large χ for both theoretical curves in Fig. 1(b).

The spectrum may also evolve from shallower than the aforementioned threshold at early times to steeper at later times. Then the influence of Rm on the saturated state could still be small, as is crudely suggested in a four-scale approach [18]. Future high-resolution simulations for both $Pm > 1$ and $Pm < 1$ are needed to concretely confirm the spectral slope of the magnetic helicity at large Rm and its temporal evolution.

To summarize, for a magnetic helicity spectrum that satisfies the conditions mentioned three paragraphs above, the Rm-independent value that \tilde{E}_L can obtain at any χ is

$$\lim_{Rm \rightarrow \infty} \tilde{E}_L(\chi, Rm) = \lim_{Rm \rightarrow \infty} T_D = -\frac{s_2}{s_1} \frac{k_1}{k_{\text{peak}}} \frac{q-2}{q-1} \chi^2, \quad (8)$$

where k_{peak} is the Rm-independent peak of the magnetic helicity spectrum and $q > 2$ is the slope at $k \geq k_{\text{peak}}$.

Eq. (8) is the lower bound for any case with finite Rm, to which the positive T_R term will additionally contribute. Since we have shown that $\tilde{\gamma}$ is asymptotically independent of Rm, it follows that the time to reach this lower bound is also Rm-independent when $Rm \rightarrow \infty$. For all of our simulation runs, we observe \tilde{E}_L is more than 12.5 times this lower bound by taking $s_1/s_2 = -1$, $k_{\text{peak}} = 2k_f$ and $q = 8/3$, again highlighting the dominance of the resistive contribution.

Furthermore, assuming $s_1/s_2 = -1$, $k_{\text{peak}} = 2k_f$, $q = 8/3$, $k_f/k_1 = 5$ and $\chi^2 = 1 - k_1/k_f$, we find this lower bound to be $E_L/u_{\text{rms}}^2 \simeq \langle B \rangle^2 / \langle b^2 \rangle = 0.032$, comparable to some observed galactic magnetic fields [44] which have benefited from the Rm-independent Ω effect and possible helicity fluxes. Hence, the DQ formalism predicts a substantial lower bound for the large-scale magnetic energy.

Conclusions.—Focusing on the PQ regime, namely the growth after the SSD saturates but before the resistive phase, our simulations and analyses reveal that: (i) For isotropically helically forced flows, the large-scale field growth rate becomes Rm-independent at modest Rm in accordance with the DQ formalism. Namely, α_k remains Rm-independent during the course of the simulation and the Lorentz-force back-reaction that ends the LSD regime exerts itself not by suppressing α_k , but by growth of α_m . (ii) In contrast, the large-scale field strength attained in the PQ regime for Rm values accessible in the simulations is Rm-dependent, being dominated by the resistive loss of magnetic helicity even for $Rm \simeq 500$. (iii) However, the same LSD analysis shows that the $Rm \rightarrow \infty$ dependence of the PQ regime depends on the evolution of the current helicity spectrum, or equivalently the magnetic helicity spectrum given the boundary conditions. For sufficiently steep magnetic helicity spectra, the regime becomes Rm-independent as $Rm \rightarrow \infty$, with the large-scale magnetic energy lower bound given by Eq. (8).

These results imply that when the current helicity spectrum falls off more steeply than k^0 , efficient LSD growth is possible in high-Rm α^2 or α^2 - Ω dynamos of stars and galaxies. This applies even without boundary helicity fluxes, although systems requiring fast cycle periods would favor helicity flux driven dynamos. For shallower spectra, helicity fluxes or some non-helicity driven LSD [e.g. 45] would be needed to explain the observed field strengths, let alone fast cycle periods. For planetary dynamos whose resistive time scales can be comparable to LSD dynamical times, α quenching is significantly weakened by resistive diffusion and so the LSD is much less constrained by the slope of the current helicity spectrum.

Finally, hyper-diffusivity is sometimes used for mimicking high-Rm flows [20]. Because the dissipation rate depends strongly on wave number, magnetic energy piles up near the resistive scale (bottleneck effect) [46]. If these resistive-scale fields are helical, k_2 becomes large and our analysis shows that the LSD growth rate is

strongly quenched even though it eventually leads to super-equipartition magnetic energies. Hence, helical LSDs with hyper-diffusion are actually less effective for inferring realistic asymptotic LSD behavior.

Nordita is sponsored by Nordforsk. We acknowledge allocation of computing resources from the Swedish National Allocations Committee at the Center for Parallel Computers at the Royal Institute of Technology in Stockholm and Linköping. EB acknowledges the Isaac Newton Institute for Mathematical Sciences, Cambridge, for support and hospitality during the programme “Frontiers in dynamo theory: from the Earth to the stars”. This work was supported by EPSRC grant no EP/R014604/1. EB acknowledges support from grants US Department of Energy DE-SC0001063, DE-SC0020432, DE-SC0020103, and US NSF grants AST-1813298, PHY-2020249.

Data and post-processing programs for this article are available on Zenodo at doi:10.5281/zenodo.7632994 [41].

-
- [1] E. N. Parker, Hydromagnetic Dynamo Models., *ApJ* **122**, 293 (1955).
- [2] M. Steenbeck, F. Krause, and K. H. Rädler, Berechnung der mittleren LORENTZ-Feldstärke für ein elektrisch leitendes Medium in turbulenter, durch CORIOLIS-Kräfte beeinflusster Bewegung, *Zeitschrift Naturforschung Teil A* **21**, 369 (1966).
- [3] H. K. Moffatt, *Magnetic field generation in electrically conducting fluids* (Cambridge University Press, 1978).
- [4] K.-H. Rädler, N. Kleeorin, and I. Rogachevskii, The Mean Electromotive Force for MHD Turbulence: The Case of a Weak Mean Magnetic Field and Slow Rotation, *Geophysical and Astrophysical Fluid Dynamics* **97**, 249 (2003), arXiv:astro-ph/0209287 [astro-ph].
- [5] K.-H. Rädler and R. Stepanov, Mean electromotive force due to turbulence of a conducting fluid in the presence of mean flow, *Physical Review E* **73**, 056311 (2006), arXiv:physics/0512120 [physics.flu-dyn].
- [6] R. M. Kulsrud and S. W. Anderson, The Spectrum of Random Magnetic Fields in the Mean Field Dynamo Theory of the Galactic Magnetic Field, *ApJ* **396**, 606 (1992).
- [7] F. Cattaneo and S. I. Vainshtein, Suppression of Turbulent Transport by a Weak Magnetic Field, *ApJL* **376**, L21 (1991).
- [8] S. I. Vainshtein and F. Cattaneo, Nonlinear Restrictions on Dynamo Action, *ApJ* **393**, 165 (1992).
- [9] A. V. Gruzinov and P. H. Diamond, Self-consistent theory of mean-field electrodynamics, *Phys. Rev. Lett.* **72**, 1651 (1994).
- [10] A. V. Gruzinov and P. H. Diamond, Self-consistent mean field electrodynamics of turbulent dynamos, *Physics of Plasmas* **2**, 1941 (1995).
- [11] A. V. Gruzinov and P. H. Diamond, Nonlinear mean field electrodynamics of turbulent dynamos, *Physics of Plasmas* **3**, 1853 (1996).
- [12] M. Ossendrijver, M. Stix, and A. Brandenburg, Magnetoconvection and dynamo coefficients: Dependence of the alpha effect on rotation and magnetic field, *A&A* **376**, 713 (2001), arXiv:astro-ph/0108274 [astro-ph].
- [13] S. M. Tobias and F. Cattaneo, Shear-driven dynamo waves at high magnetic Reynolds number, *Nature* **497**, 463 (2013).
- [14] A. Pouquet, U. Frisch, and J. Leorat, Strong MHD helical turbulence and the nonlinear dynamo effect, *Journal of Fluid Mechanics* **77**, 321 (1976).
- [15] N. Kleeorin and A. Ruzmaikin, Dynamics of the average turbulent helicity in a magnetic field, *Magnetohydrodynamics* **18**, 116 (1982).
- [16] E. G. Blackman and G. B. Field, Constraints on the Magnitude of α in Dynamo Theory, *ApJ* **534**, 984 (2000), arXiv:astro-ph/9903384 [astro-ph].
- [17] E. G. Blackman and G. B. Field, New Dynamical Mean-Field Dynamo Theory and Closure Approach, *Phys. Rev. Lett.* **89**, 265007 (2002), arXiv:astro-ph/0207435 [astro-ph].
- [18] E. G. Blackman, Understanding helical magnetic dynamo spectra with a non-linear four-scale theory, *MNRAS* **344**, 707 (2003), arXiv:astro-ph/0301432 [astro-ph].
- [19] A. Brandenburg, K.-H. Rädler, M. Rheinhardt, and K. Subramanian, Magnetic Quenching of α and Diffusivity Tensors in Helical Turbulence, *ApJL* **687**, L49 (2008), arXiv:0805.1287 [astro-ph].
- [20] A. Brandenburg and G. R. Sarson, Effect of Hyperdiffusivity on Turbulent Dynamos with Helicity, *Phys. Rev. Lett.* **88**, 055003 (2002), arXiv:astro-ph/0110171 [astro-ph].
- [21] S. Candelaresi and A. Brandenburg, Kinetic helicity needed to drive large-scale dynamos, *Physical Review E* **87**, 043104 (2013), arXiv:1208.4529 [astro-ph.SR].
- [22] E. T. Vishniac and J. Cho, Magnetic Helicity Conservation and Astrophysical Dynamos, *ApJ* **550**, 752 (2001), arXiv:astro-ph/0010373 [astro-ph].
- [23] K. Subramanian and A. Brandenburg, Nonlinear Current Helicity Fluxes in Turbulent Dynamos and

- Alpha Quenching, *Phys. Rev. Lett.* **93**, 205001 (2004), arXiv:astro-ph/0408020 [astro-ph].
- [24] A. Hubbard and A. Brandenburg, Catastrophic Quenching in $\alpha\Omega$ Dynamos Revisited, *ApJ* **748**, 51 (2012), arXiv:1107.0238 [astro-ph.SR].
- [25] F. Rincon, Helical turbulent nonlinear dynamo at large magnetic Reynolds numbers, *Physical Review Fluids* **6**, L121701 (2021), arXiv:2108.12037 [physics.flu-dyn].
- [26] K. Gopalakrishnan and K. Subramanian, Magnetic helicity fluxes from triple correlators, arXiv e-prints, arXiv:2209.14810 (2022), arXiv:2209.14810 [astro-ph.GA].
- [27] P. Bhat, Saturation of large-scale dynamo in anisotropically forced turbulence, *MNRAS* **509**, 2249 (2022), arXiv:2108.08740 [astro-ph.SR].
- [28] A. Brandenburg and K. Subramanian, Astrophysical magnetic fields and nonlinear dynamo theory, *Physics Reports* **417**, 1 (2005), arXiv:astro-ph/0405052 [astro-ph].
- [29] A. Brandenburg, Advances in mean-field dynamo theory and applications to astrophysical turbulence, *Journal of Plasma Physics* **84**, 735840404 (2018), arXiv:1801.05384 [physics.flu-dyn].
- [30] D. W. Hughes, Mean field electrodynamics: triumphs and tribulations, *Journal of Plasma Physics* **84**, 735840407 (2018), arXiv:1804.02877 [astro-ph.SR].
- [31] F. Rincon, Dynamo theories, *Journal of Plasma Physics* **85**, 205850401 (2019), arXiv:1903.07829 [physics.plasm-ph].
- [32] A. Brandenburg and E. Ntormousi, Galactic Dynamos, arXiv e-prints, arXiv:2211.03476 (2022), arXiv:2211.03476 [astro-ph.GA].
- [33] K. Subramanian, Unified Treatment of Small and Large-Scale Dynamos in Helical Turbulence, *Phys. Rev. Lett.* **83**, 2957 (1999), arXiv:astro-ph/9908280 [astro-ph].
- [34] S. Boldyrev, F. Cattaneo, and R. Rosner, Magnetic-Field Generation in Helical Turbulence, *Phys. Rev. Lett.* **95**, 255001 (2005), arXiv:astro-ph/0504588 [astro-ph].
- [35] P. Bhat, K. Subramanian, and A. Brandenburg, A unified large/small-scale dynamo in helical turbulence, *MNRAS* **461**, 240 (2016), arXiv:1508.02706 [astro-ph.GA].
- [36] J. Pietarila Graham, E. G. Blackman, P. D. Mininni, and A. Pouquet, Not much helicity is needed to drive large-scale dynamos, *Physical Review E* **85**, 066406 (2012), arXiv:1108.3039 [physics.flu-dyn].
- [37] P. Bhat, K. Subramanian, and A. Brandenburg, Efficient quasi-kinematic large-scale dynamo as the small-scale dynamo saturates, arXiv e-prints, arXiv:1905.08278 (2019), arXiv:1905.08278 [astro-ph.GA].
- [38] A. Brandenburg, The Inverse Cascade and Nonlinear Alpha-Effect in Simulations of Isotropic Helical Hydromagnetic Turbulence, *ApJ* **550**, 824 (2001), arXiv:astro-ph/0006186 [astro-ph].
- [39] G. Bermudez and A. Alexakis, Saturation of Turbulent Helical Dynamos, *Phys. Rev. Lett.* **129**, 195101 (2022), arXiv:2204.14091 [physics.flu-dyn].
- [40] Pencil Code Collaboration, A. Brandenburg, A. Johansen, P. Bourdin, W. Dobler, W. Lyra, M. Rheinhardt, S. Bingert, N. Haugen, A. Mee, F. Gent, N. Babkovskaia, C.-C. Yang, T. Heinemann, B. Dinttrans, D. Mitra, S. Candelaresi, J. Warnecke, P. Käpylä, A. Schreiber, P. Chatterjee, M. Käpylä, X.-Y. Li, J. Krüger, J. Aarnes, G. Sarson, J. Oishi, J. Schober, R. Plasson, C. Sandin, E. Karchniwy, L. Rodrigues, A. Hubbard, G. Guerrero, A. Snodin, I. Losada, J. Pekkila, and C. Qian, The Pencil Code, a modular MPI code for partial differential equations and particles: multipurpose and multiuser-maintained, *The Journal of Open Source Software* **6**, 2807 (2021), arXiv:2009.08231 [astro-ph.IM].
- [41] H. Zhou and E. Blackman, Dataset for “Helical dynamo growth at modest versus extreme magnetic Reynolds numbers”, 10.5281/zenodo.7632994 (2023), Zenodo.
- [42] H. Zhou and E. Blackman, Supplemental Material for the manuscript “Helical dynamo growth at modest versus extreme magnetic Reynolds numbers”, (2023).
- [43] A. K. Galishnikova, M. W. Kunz, and A. A. Schekochihin, Tearing Instability and Current-Sheet Disruption in the Turbulent Dynamo, *Physical Review X* **12**, 041027 (2022), arXiv:2201.07757 [astro-ph.HE].
- [44] R. Beck, L. Chamandy, E. Elson, and E. G. Blackman, Synthesizing Observations and Theory to Understand Galactic Magnetic Fields: Progress and Challenges, *Galaxies* **8**, 4 (2019), arXiv:1912.08962 [astro-ph.GA].
- [45] V. Skoutnev, J. Squire, and A. Bhattacharjee, On large-scale dynamos with stable stratification and the application to stellar radiative zones, *MNRAS* **517**, 526 (2022), arXiv:2203.01943 [astro-ph.SR].
- [46] D. Biskamp, E. Schwarz, and A. Celani, Non-local Bottleneck Effect in Two-Dimensional Turbulence, *Phys. Rev. Lett.* **81**, 4855 (1998), arXiv:chao-dyn/9807012 [nlin.CD].